3D Question Answering for City Scene Understanding

Anonymous Author(s)

ABSTRACT

3D multimodal question answering (MQA) plays a crucial role in scene understanding by enabling intelligent agents to comprehend their surroundings in 3D environments. While existing research has primarily focused on indoor household tasks and outdoor roadside autonomous driving tasks, there has been limited exploration of city-level scene understanding tasks. Furthermore, existing research faces challenges in understanding city scenes, due to the absence of spatial semantic information and human-environment interaction information at the city level. To address these challenges, we investigate 3D MQA from both dataset and method perspectives. From the dataset perspective, we introduce a novel 3D MQA dataset named **City-3DQA** for city-level scene understanding, which is the first dataset to incorporate scene semantic and human-environment interactive tasks within the city. From the method perspective, we propose a **S**cene **g**raph enhanced **City**-level **U**nderstanding method (**Sg-CityU**), which utilizes the scene graph to introduce the spatial semantic. A new benchmark is reported and our proposed Sg-CityU achieves accuracy of 63.94% and 63.76% in different settings of City-3DQA. Compared to indoor 3D MQA methods and zero-shot using advanced large language models (LLMs), Sg-CityU demonstrates state-of-the-art (SOTA) performance in robustness and generalization. Our dataset and code are available on our project website[1].

CCS CONCEPTS

• **Computing methodologies → Natural language processing**; **Scene understanding**.

KEYWORDS

multimodal question answering, scene understanding, 3D

1 INTRODUCTION

City scene understanding is a crucial technology for guided tour [40], autonomous systems [15], and smart city [7]. 3D multimodal question answering (MQA) is one of the key manners of human-environment interaction to promote city scene understanding [23]. For instance, people with visual impairment could interact with the electronic personal assistant (seen as an agent) integrated into wearable smart glasses, such as Microsoft HoloLens [2] or Apple Vision Pro [1], to obtain auxiliary scenario information in the situated city by asking questions with city perception from the embedded visual sensors, shown in Figure 1 (c).

[1]https://sites.google.com/view/city3dqa/

ACM MM, 2024, Melbourne, Australia

ACM ISBN 978-1-4503-XXXX-X/18/06
https://doi.org/XXXXXXX.XXXXXXX

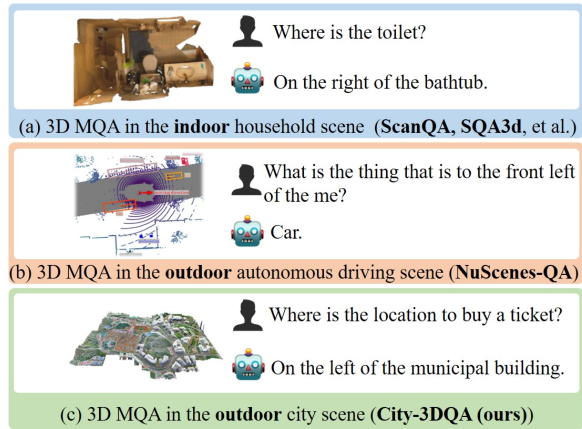

Figure 1: Comparison of the City-3DQA with other 3D multimodal question answering (MQA) tasks. The existing research in 3D MQA focuses on the indoor household scene (a) and outdoor autonomous driving scene (b). However, these researches lack spatial semantic and city-level interaction information within the city. City-3DQA (c) is the first dataset to focus on 3D MQA for outdoor city scene understanding.

However, existing 3D MQA tasks face challenges in city scene understanding due to lacking spatial semantic information and city-level interaction information within the city, such as the location and the usage of instances. Existing research mainly focuses on two lines including the 3D MQAs in the indoor household setting (Fig. 1 (a)) and the 3D MQAs in the outdoor autonomous driving settings(Fig. 1 (b)). For the former, EQA [10], MP3D-EQA [42], MT-EQA [48] and EMQA [11] realize MQA-based scene understanding using images in indoor household scenarios through House3D simulation environment [43] for navigation tasks. Apart from using images, there is also 3D MQA research, such as 3DQA [47], ScanQA [4], CLEvR3D [45], FE-3DGQA [50] and SQA3D [28], which adopt point cloud for indoor household scene understanding based on the point cloud environment ScanNet [9]. For the latter, Qian et al. [33] introduce NuScenes-QA in outdoor settings firstly for autonomous driving using the point cloud. This task focuses on roadside-related instances including cars and pedestrians, yet it does not consider other instances in the city such as *plantings*, *buildings*, and *rivers*. In summary, current 3D MQAs are hard to satisfy city-level scene understanding for urban activities of humans or agents.

To address these challenges, we explore the task from both the dataset and method perspectives. From the dataset perspective, we introduce **City-3DQA**, the first 3D MQA dataset for outdoor city scene understanding in Figure 2. We realize data collection including City-level Instance Segmentation, Scene Semantic Extraction, and Question-Answer Pair Construction. Specifically, in City-level

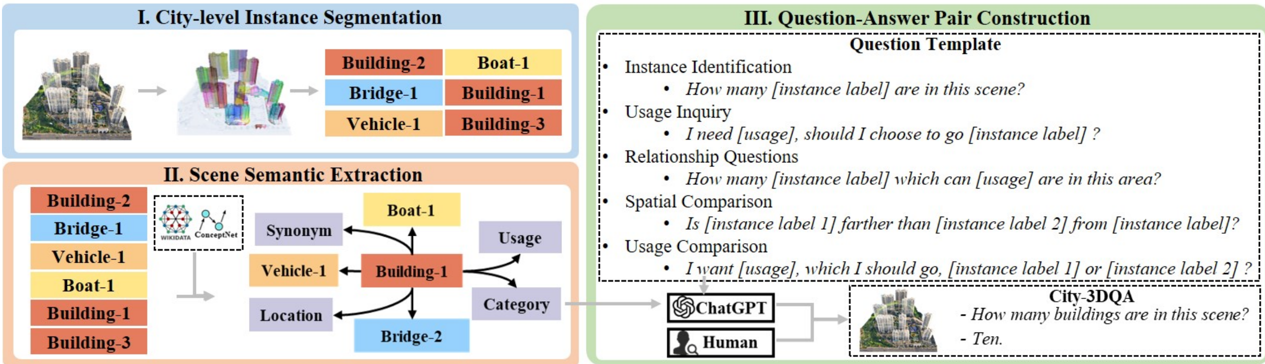

Figure 2: Data Construction Pipeline for City-3DQA. The pipeline consists of three main stages: City-level Instance Segmentation, Scene Semantic Extraction, and Question-Answer Pair Construction.

Instance Segmentation, we utilize pre-trained instance segmentation models to identify city instances. In Scene Semantic Extraction, we construct the scene semantic information for instances in the graph structure, including spatial information and semantic information. The spatial information denotes relationships between pairs of instances, such as "*living building - left - business building*". The semantic information represents instances with attributes, such as "*transportation building - usage - buying tickets*". In Question-Answer Pair Construction, we develop 33 unique question templates that enable multi-hop reasoning and urban activities, which are classified into five categories: instance identification, usage inquiry, relationship questions, spatial comparison, and usage comparison for the city scene understanding inspired by Gao et al. [13] and Qian et al. [33]. The LLM leverages these templates in combination with scene semantic information to produce question-answer pairs. The human evaluation assesses dataset quality. The City-3DQA dataset comprises **450k question-answer pairs** and 2.5 **billion point clouds** across six cities.

From the method perspective, we introduce a **S**cene **g**raph enhanced **City**-level **U**nderstanding method (**Sg-CityU**) for City-3DQA. Compared to indoor scene understanding, city-level scene understanding is limited by sparse semantic information due to large scales. This leads to challenges associated with long-range connections and spatial inference during the modeling process [25]. Therefore, Sg-CityU utilizes the scene graph to introduce spatial relationship information among instances. Specifically, for the input point cloud and the question, Sg-CityU extracts the vision and language representation from point clouds and questions respectively. And then a city-level scene graph is constructed, which is encoded through graph neural networks [20, 21]. We design the Fusion Layer to fuse aforementioned scene representations for answering generation.

Our main contributions can be summarized as follows:

(1) We investigate 3D multimodal question answering (MQA) to realize city-level scene understanding for urban activities of humans or agents.
(2) We introduce a novel large-scale dataset named City-3DQA. To our knowledge, City-3DQA is the first dataset to consider scene semantic information and city-level interactive tasks.
(3) We provide a baseline method (**Sg-CityU**), which introduces spatial relationship information through the scene graph to generate high-quality city-related answers.
(4) A new benchmark is proposed in which evaluations are conducted with existing MQA methods and LLM-based zero-shot methods on our City-3DQA. Experimental results show that our proposed **Sg-CityU** achieves the best performance in robustness and generalization, specifically, 63.94% and 63.76% accuracy in sentence-wise and city-wise settings respectively.

2 RELATED WORK

2.1 City Scene Understanding

Existing research in city scene understanding primarily concentrates on segmentation, reconstruction, and grounding. City segmentation, as explored in works such as Geng et al. [14], Hu et al. [17], Liao et al. [25], Yang et al. [46], aims to distinguish different instances within city-level point clouds or meshes for a comprehensive understanding of urban environments. City scene reconstruction, as discussed in Kuang et al. [22], Lin et al. [26], Tang et al. [37], Zhang et al. [49], seeks to understand the visual information of each object in city scenes and reconstruct their geometries from partial observations, such as point clouds from 3D scans. However, these methods primarily focus on visual representation rather than language representation and semantic information in city scenes, which are important for human-environment interaction. Miyanishi et al. [29] introduce CityRefer, which addresses city-level visual grounding by localizing objects in 3D scenes based on language expressions. Inspired by these studies, our research aims to tackle this problem from a multimodal question answering perspective. We propose the first 3D multimodal question answering dataset, City-3DQA, for 3D city scene understanding, which integrates language representation and semantic information.

2.2 3D Multimodal Question Answering

3D Multimodal Question Answering is a novel task within the field of scene understanding, concentrating on the ability to answer questions about 3D scenes, which are depicted through simulated environments or point clouds [4]. Das et al. [10], Datta et al.

[11], Wijmans et al. [42], Yu et al. [48] present an embodied question answering where the agent must first intelligently navigate to explore the environment, gather the necessary visual information through first-person vision, and then respond to the question in a 3D simulated environment. Azuma et al. [4], Etesam et al. [12], Ma et al. [28], Yan et al. [45], Ye et al. [47], Zhao et al. [50] propose a series of studies based on the ScanNet dataset [9] that focus on processing point cloud data from entire 3D indoor scenes to respond to specific textual queries about the environment. However, these works focus on the indoor household scene and overlook the outdoor scene. Qian et al. [33] proposes the outdoor 3D multimodal question NuScenes-QA answering benchmark to address the human-machine interaction in autonomous driving rather than the city scene understanding. We first introduce City-3DQA, a 3D question-answering dataset specifically designed for the understanding of outdoor city scenes. Unlike the NuScenes-QA which concentrates on roadside areas, City-3DQA emphasizes the comprehension of city landscapes along with their spatial characteristics. Additionally, it incorporates features related to interaction, such as usage.

3 PROBLEM DEFINITION

The 3D MQA for city scene understanding is formulated as follows: given inputs of the point cloud p and question q about the 3D city scene, the model aims to output $\widehat{a}$ that semantically matches true answer a^* from the answer set $\mathbb{A}$,

$$\widehat{a} = \arg\max_{a \in \mathbb{A}} \mathrm{P}(a|p, q). \tag{1}$$

Understanding city-level scenes is more challenging than indoor scenes. This is because city scenes have less dense information over large areas, making it hard to model long-range connections and spatial relationships [25]. Therefore, we introduce a scene graph sg which contains the relative spatial relationship [44]. The sg is composed of nodes and edges, where the nodes represent instances and the edges represent the spatial relationships between these instances. We consider a scene-graph-aware joint probability model for the task using sg and decompose Equation 1 into two parts, given by:

$$\mathrm{P}(a|p, q) = \mathrm{P}(a|p, q, sg) \times \mathrm{P}(sg|p). \tag{2}$$

4 CITY-3DQA DATASET

4.1 Data Construction

We develop an automatic pipeline for the construction of the City-3DQA dataset, as depicted in Figure 2. The City-3DQA dataset is derived from the 3D city point cloud dataset UrbanBIS [46]. Our pipeline encompasses three primary components: City-level Instance Segmentation, Scene Semantic Extraction, and Question-Answer Pair Construction.

City-level Instance Segmentation. We use pre-trained instance segmentation [46] for the UrbanBIS dataset and obtain a wide range of city instances including buildings, vehicles, vegetation, roads, and bridges covering six cities, Qingdao, Wuhu, Longhua, Yuehai, Lihu, and Yingrenshi. We extract the instance-level label along with annotations and spatial locations to build the instance set $S_I = \{i, (x_i, y_i, z_i) | i \in I\}$ from UrbanBIS, where I is the instances from the raw dataset. x_i, y_i, z_i is the x-axis, y-axis, and z-axis coordinate for each i.

Scene Semantic Extraction. We construct the scene semantic information G_i for each instance i in the graph structure, which comprises two components: the spatial information sp_i and the semantic information se_i in the graph structure. sp_i contains a series triples $(i, r^{sp}_{i,j}, j)$, where $r^{sp}_{i,j}$ is the spatial relationship between the instances (i, j), where $i \in S_I, j \in S_I$. These relationships are centered around instance i and we define counterclockwise as the positive direction. $R_{i,j}$ are divided via eight relationships: "*front*", "*front-right*", "*right*", "*back-right*", "*front-left*", "*left*", "*back-left*" and "*back*", depending on relative instance spatial positions and the angle between instance i and j,

$$\theta = \arctan \frac{y_j - y_i}{x_j - x_i},$$
$$r^{sg}_{i,j} = \begin{cases} \text{front} & \text{if} - 22.5^\circ < \theta \le 22.5^\circ \\ \text{front-right} & \text{if } 22.5^\circ < \theta \le 67.5^\circ \\ \text{right} & \text{if } 67.5^\circ < \theta \le 112.5^\circ \\ \text{back-right} & \text{if } 112.5^\circ < \theta \le 157.5^\circ \\ \text{front-left} & \text{if } -67.5^\circ < \theta \le -22.5^\circ \\ \text{left} & \text{if } -112.5^\circ < \theta \le -67.5^\circ \\ \text{back-left} & \text{if } -157.5^\circ < \theta \le -112.5^\circ \\ \text{back} & \text{else .} \end{cases} \tag{3}$$

se_i are defined as triples (i, r^{se}_i, v_i), where r^{se}_i and v_i are the attribute and value for instance i respectively. In City-3DQA, we define r^{se}_i as five attributes including instance label, building category label, synonym label, location, and usage label. The instance label and a detailed building category label are sourced from the pre-trained instance segmentation method [46]. Drawing inspiration from Henderson et al. [16], we acknowledge the usage label as an important aspect of urban activities within the city scene. To enhance the relevance of the City-3DQA datasets to a common language and to promote linguistic variety, we integrate synonyms, as suggested by [35]. The sources for usage descriptions and synonym labels are knowledge base WikiData [39] and ConceptNet [36].

Question-Answer Pair Construction. To construct the question-answer pairs automatically, we propose a template-based pipeline utilizing LLM to transform structured data G_i into unstructured language question q_i and answer a_i for the instance i. In our study, we formulate two distinct questions using the G_i within the City-3DQA framework. The first question aims to extract the tail j in $sp_i = \{i, r^{sp}_{i,j}, j\}$ or the value v_i in $se_i = \{i, r^{se}_i, v_i\}$, to build the answer in the question-answer pair. The second question concentrates on identifying the edge between the tail and head of a triplet, such as the relationship $r^{sp}_{i,j}$ in $sp_i = \{i, r^{sp}_{i,j}, j\}$ or the attribute r^{se}_i in $se_i = \{i, r^{se}_i, v_i\}$, to formulate the answer in the question-answer pair.

Building upon the work of Gao et al. [13] and Qian et al. [33], the City-3DQA dataset is comprised of 33 question templates, which are categorized into five categories: instance identification, usage inquiry, relationship questions, spatial comparison, and usage comparison. These templates are detailed in the supplementary material. The first three categories of templates are designed to evaluate the presence, quantity, and characteristics of instances within city

Table 1: Comparison between City-3DQA and other 3D MQA datasets. Question-Answer Pairs and Point Clouds denote the number of question-answer pairs and points.

Dataset	Scene	Collection	Scale	Input Modal	Question-Answer Pairs	Point Clouds
EQA [10]	indoor	template	Room	image	1.5k	-
MP3D-EQA [42]	indoor	template	Room	image	1.1k	-
EMQA [11]	indoor	human	Room	image	9.7k	-
MT-EQA [48]	indoor	template+human	Room	image	19k	-
3DVQA [12]	indoor	template	Room	point cloud	484k	242M
3DQA [47]	indoor	human	Room	point cloud	10k	242M
ScanQA [4]	indoor	auto + human	Room	point cloud	41k	242M
CLEVR3D [45]	indoor	template	Room	point cloud	60.1k	242M
FE-3DGQA [50]	indoor	human	Room	point cloud	20k	242M
SQA3D [28]	indoor	human	Room	point cloud + image	33.4k	242M
NuScenes-QA [33]	outdoor	template	Roadside	point cloud + image	460k	1.4B
City-3DQA (ours)	outdoor	template + auto + human	City	point cloud	450k	2.5B

scenes, including their usages and relationships and urban activities. These templates necessitate straightforward answers and are categorized as single-hop questions. For example, questions such as "*What is the usage of [instance label]?*" and "*Where is [instance label]?*" are formulated. To facilitate the construction of these questions, we employ slots like "*[instance label]*", "*[location]*", and "*[usage]*" for completion by LLMs. The last two categories of templates are designed to evaluate the comparison of instances within city scenes, including their usages and relationships. These templates necessitate a multi-hop reasoning step to arrive at the answer and they are classified into multi-hop questions For instance, inquiries such as "*I want [usage], which I should go, [instance label 1] or [instance label 2] ?*" and "*Between [instance label 1] and [instance label 2], which is nearest to [instance label]?*" are devised. We utilize slots such as "*[instance label 1]*" and "*[instance label 2]*" in the templates for the comparative analysis of instances in the city.

We design the prompt function $f_{prompt}(\cdot)$ which incorporates slots. The details of the prompt are shown in the supplementary material. These slots are populated using the input G_i. We utilize the ChatGPT API with the gpt-3.5-turbo model. The whole pipeline can be formulated as below:

$$(q_i, a_i) = search\ \mathrm{LLM}(f_{prompt}(G_i)), \tag{4}$$

where the search function $search(\cdot)$ could be an argmax function that searches for the highest-scoring output or sampling that randomly generates outputs following the probability distribution of the adopted LLM. The prompt engineering $f_{prompt}(\cdot)$ is detailed in the supplementary material. The LLM combination with templates offers linguistic diversity and improves the quality of the corpus compared to using templates alone [41]. After the automated generation of question-answer pairs by LLMs, we conduct the human evaluation to assess and guarantee the quality and accuracy of the City-3DQA dataset.

4.2 Data Statistics

In the vision modal, City-3DQA covers 193 unique city scenes across six cities including Qingdao, Wuhu, Longhua, Yuehai, Lihu, and Yingrenshi, incorporating **2.5 billion** point clouds. The combined coverage of these scenes extends over an area of 10.78 square kilometers. The dataset includes information from **3, 370** instances of various city instances such as buildings, bridges, vehicles, and boats. The comparison between City-3DQA and other 3D MQA works is shown in Table 1.

In the language modal, the City-3DQA dataset comprises **450k** question-answer pairs covering five different questions in city scene understanding including instance identification, usage inquiry, relationship questions, spatial comparison, and usage comparison. Figure 3 illustrates the basic statistics of our dataset of language modal. In Figure 3(a), the distribution of question types in the dataset is as follows: usage inquiry (5.6%), instance identification (6.3%), relationship question (35.3%), spatial comparison (32.5%), and usage comparison (20.3%). Furthermore, the dataset comprises 47.2% single-hop questions and 52.8% multi-hop questions. Figure 3(b) demonstrates that the lengths of our questions vary significantly, ranging from five to twenty-five words. Figure 3(c) presents a visualization of the extensive vocabulary employed in the questions of our dataset.

5 METHOD

We propose a framework to model Equation 2, named **Sg-CityU** (**S**cene **g**raph enhanced **City**-level **U**nderstanding) method shown in Figure 4 (a). Sg-CityU model consists of Multimodal Encoder, Fusion Layer, and Answer Layer.

5.1 Multimodal Encoder

We use the input point cloud p consisting of point coordinates $c \in \mathbb{R}^3$ in the 3D space for 3D representation. Following previous 3D and language research, we use additional point features such as the height of the point, colors, and normals [4, 8]. Sg-CityU detects objects in the scene based on point cloud features using VoteNet [31], which uses PointNet++ [32] as a backbone network. We get object proposals from VoteNet for the instances and the whole scan and project them through the multi-layer perceptron (MLP) to obtain the object proposal representation,

$$F_p = \mathrm{MLP}(\mathrm{VoteNet}(i_p)), \tag{5}$$

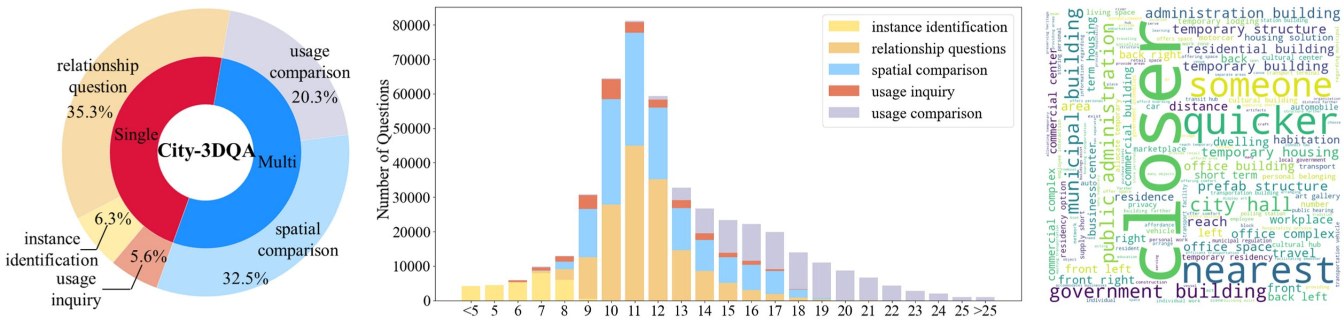

(a) Question Distribution

(b) Question Length Distribution

(c) Question Word Cloud

Figure 3: The statistical distributions of questions within the City-3DQA dataset are presented. The question length means the number of words in the question sentence. Multi and Single mean the multi-hop questions and single-hop questions respectively.

where $F_p \in \mathbb{R}^{dim \times N}$ and i_p is the point cloud for the instances. dim represents the hidden size of representation, and n indicates the number of proposals. A question sentence q is fed to the pre-trained language model encoder BERT [19] and MLP to calculate the question features $F_q \in \mathbb{R}^{dim}$,

$$F_q = \mathrm{MLP}(\mathrm{BERT}(q)). \tag{6}$$

We construct the sg based on i_p to introduce spatial relationship among i_p. The sg comprises nodes, which represent instances, and edges, which denote the spatial relationships between these instances. The relationships are divided and defined as Equation 3. We encode sg through n-layers graph convolutional networks (GCN) [21] and output the representation $F_{sg} \in \mathbb{R}^{dim \times N}$,

$$\begin{aligned} sg^{m+1} &= \mathrm{GCN}^m(sg^m), \\ F_{sg} &= \mathrm{MLP}(sg^{m+1}), \end{aligned} \tag{7}$$

where GCN^m is the learnable GCNs at the m-th layer, and F_{sg} is the feature of the node after encoding by m-th GCN layer. Inspired by language model type condition [24], we initialize sg^0 with the word embeddings of the nodes and edges.

5.2 Fusion Layer

In the Fusion Layer, we design the multimodal fusion network (MMFN) for the different inputs as shown in Figure 4 (b). Specifically, MMFN consists of self-attention and cross-attention and takes F_p, F_q, F_{sg} as input,

$$\begin{aligned} F_q &= \text{Self-Attention}(F_q), \\ F_p &= \text{Self-Attention}(F_p), \\ F_p &= \text{Cross-Attention}(F_p, F_q), \\ F_{sg} &= \text{Self-Attention}(F_{sg}), \\ F_{sg} &= \text{Cross-Attention}(F_p, F_{sg}), \end{aligned} \tag{8}$$

We perform the fusion multimodal features through the Fusion Layers consisting of l-th MMFN layer cascaded in depth,

$$F_p^l, F_q^l, F_{sg}^l = \mathrm{MMFN}^l(F_p^{l-1}, F_q^{l-1}, F_{sg}^{l-1}), \tag{9}$$

For MMFN^0, we set its input features $F_p^0 = F_p$, $F_q^0 = F_q$, $F_{sg}^0 = F_{sg}$, respectively.

Table 2: Different split in City-3DQA. It denotes the number of question-answer pairs and cities in different set in the split mode.

Split	train			val			test		
	Single	Multi	All	Single	Multi	All	Single	Multi	All
Sentence-wise	173k	136k	310k	34k	44k	78k	35k	26k	61k
City-wise	176k	133k	310k	37k	41k	78k	35k	26k	61k

5.3 Answer Layer

We map the fused features to the answer set $\mathbb{A}$ that matches the true answer for answer prediction with MLP,

$$F_f = \mathrm{MLP}(\mathrm{Concat}(F_p^l, F_q^l, F_{sg}^l)), \tag{10}$$

where $\mathrm{Concat}(\cdot)$ is the concatenation and $F_f \in \mathbb{R}^{dim_A \times dim}$, dim_A is the dimension of the answer set $\mathbb{A}$. To consider multiple answers, we compute final scores with the cross-entropy (CE) loss function to train the module.

6 EXPERIMENT

6.1 Implementation Details

Data Organization. To train and evaluate our proposed models, we split our City-3DQA dataset using two different modes: sentence-wise and city-wise. In the city-wise split, we categorize the examples by city. This results in four cities (Longhua, Wuhu, Qingdao, Yingrenshi) being allocated to the training set, one city (Lihu) to the validation set, and one city (Yuehai) to the test set. For the sentence-wise split, we divide the 450K question-answer pairs in City-3DQA into training, validation, and test sets with the same ratio as the city-wise split respectively and each set contains the six cities. The distribution of examples in each set, according to these splits, is detailed in Table 2.

Training Details. We employ the Adam optimizer with weight decay $5e^{-4}$, a learning rate of $1e^{-3}$, and a batch size of 50 during the training stage. Experiments are implemented with CUDA 11.2 and PyTorch 1.7.1 and run on an NVIDIA RTX A6000.

Metrics. We adopt the Top-1 accuracy (Top@1) and Top-10 accuracy (Top@10) as our evaluation metric, following the practice of

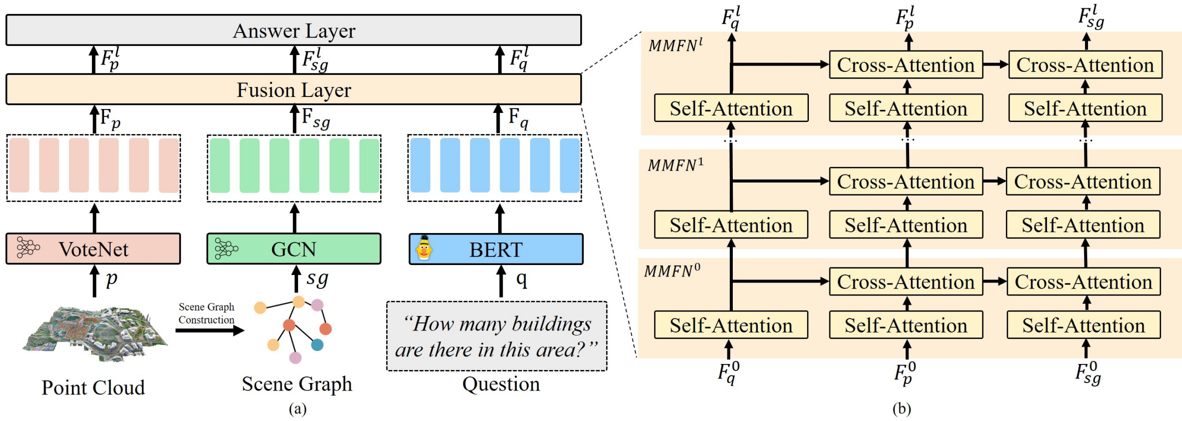

Figure 4: The framework of our proposed model Sg-CityU (a) and Fusion Layer in Sg-CityU (b). In Sg-CityU, the question, scene graph, and point clouds are processed by the feature extraction backbone to obtain multimodal features. Finally, the multimodal features are fed into Fusion Layer and Answer Layer for answer generation. In Fusion Layer, we build layers of multimodal fusion network (MMFN) based on self-attention and cross-attention to fuse different model inputs.

many other MQA methods [3, 4], and evaluate the performance of different question types separately.

Baselines. We design two categories of baselines for comparison in City-3DQA:

- **General LLMs.** We utilize LLM as baselines into two types: multimodal LLM utilizing 2D images and LLM utilizing scene graphs as input. For the former, we convert the input point clouds into 2D images. This process ensures alignment with the requirements of multimodal LLMs using 2D image input following Ma et al. [28]. Our selected baselines for this category include Qwen-VL [6], and LLaVA [27]. For the latter, we construct the scene graph from each city scene and we organize these scene graphs in language. Our selected baselines for this category include Qwen [5], and Llama-2 [38]. LLMs generate answers based on the questions and input and we select the most similar answers from answer spaces $\mathbb{A}$ based on the BERT score [34]. The prompt engineering used in LLM evaluation is detailed in supplementary material.
- **Indoor Models.** We choose the baseline models ScanQA, CLIP-Guided, 3D-VLP, and the state-of-the-art (SOTA) model 3D-VisTA using in indoor 3D MQA datasets ScanQA [4] and transfer it from indoor setting into outdoor setting. These models take point cloud as input and our model Sg-CityU takes point cloud and scene graph as input.

6.2 Results Analysis

6.2.1 ***Comparison with General LLMs.*** We compare our proposed models with the LLMs in zero-shot setting in Table 3 and our proposed model Sg-CityU outperforms in all metrics. For multimodal LLM using the projection image as input, Qwen-VL [6] demonstrates the acc@1 of 18.81% and 19.75% across all sets for sentence-wise and city-wise evaluation, respectively. Furthermore, it achieves the acc@10 of 63.86% and 63.71% in the same respective categories. On the other hand, LLaVA [27] attains an acc@1 of 20.60% and 20.56% for sentence-wise and city-wise evaluation, respectively, and an acc@10 of 67.37% and 67.02% in the corresponding test sets. Compared to the best results in multimodal LLM, Sg-CityU achieves more than 3.1 times improvement in sentence-wise (20.60% $\longrightarrow$ 63.94%) and city-wise (20.56% $\longrightarrow$ 63.76%) in acc@1 and 1.4 times improvements in sentence-wise (67.37% $\longrightarrow$ 98.81%) and city-wise (67.02% $\longrightarrow$ 98.68%) in acc@10. We attribute the poor performance of multimodal LLM to two points. First, in the zero-shot setting of multimodal LLMs, there is a lack of parameters to bridge the domain gap between the pre-trained domain and the City-3DQA domain through fine-tuning. Second, the projection image fails to accurately represent the city scene in point cloud.

For LLM using the scene graph as input, Qwen [5] achieves 30.35% and 31.31% of acc@1 in sentence-wise and city-wise, 73.84% and 75.26% of acc@10 in sentence-wise and city-wise. Llama-2 [38] achieves 37.66% and 38.37% of acc@1 in sentence-wise and city-wise, 80.02% and 79.34% of acc@10 in sentence-wise and city-wise. Compared to multimodal LLMs, LLMs with scene graphs achieve better performance and we attribute it to the LLM generalization performance in the language. Compared to the best results in LLM, Sg-CityU achieves more than 20% points improvement in sentence-wise (37.66% $\longrightarrow$ 63.94%) and city-wise (38.37% $\longrightarrow$ 63.76%) in acc@1 and over 10% points improvements in sentence-wise (80.02% $\longrightarrow$ 98.81%) and city-wise (79.34% $\longrightarrow$ 98.68%) in acc@10. The suboptimal performance of LLMs can be attributed to two points. First, due to the context window length restriction, the language input based on the scene graph can only cover part representation, constraining the understanding of the city-level scene. In a city scene comprising n instances, the corresponding scene graph contains $\frac{n(n+1)}{2}$ triples. The context windows of Llama-2 and Qwen are $4k$ and over 25% input sentences with scene graphs are over the the window sizes. Second, LLMs overlook the visual features present in city scenes, which are beneficial for the performance of 3D MQA tasks.

Table 3: The comparison between our model and different methods. We compare eight different methods with Sg-CityU and Sg-CityU achieves the best score in all metrics compared to the methods. The scene graphs are organized as language.

Category	Models	Input	Sentence-wise						City-wise					
			Single-hop		Multi-hop		All		Single-hop		Multi-hop		All	
			acc@1	acc@10	acc@1	acc@10	acc@1	acc@10	acc@1	acc@10	acc@1	acc@10	acc@1	acc@10
General LLMs	Qwen-VL [6]	Image	30.53	70.85	9.76	58.45	18.81	63.86	30.79	71.07	9.78	57.07	19.75	63.71
	LLaVA [27]	Image	33.93	77.02	10.33	59.92	20.60	67.37	32.56	76.94	9.84	58.07	20.56	67.02
	Qwen [5]	Scene Graph	55.25	85.41	11.21	63.48	30.35	73.84	55.40	85.49	12.59	66.35	31.31	75.26
	Llama-2 [38]	Scene Graph	60.51	86.34	20.00	75.13	37.66	80.02	60.03	86.18	18.82	73.17	38.37	79.34
Indoor Models	ScanQA [4]	Point Cloud	76.42	90.75	28.31	86.46	49.28	88.34	64.84	88.73	27.03	84.37	47.33	86.45
	CLIP-Guided [30]	Point Cloud	74.54	98.49	33.73	97.54	51.55	98.38	63.05	98.35	32.41	97.12	46.94	98.00
	3D-VLP [18]	Point Cloud	72.78	98.55	35.54	97.76	51.72	98.40	64.03	98.42	34.95	97.19	48.74	98.33
	3D-VisTA [51]	Point Cloud	79.23	98.52	44.67	97.85	59.63	98.37	71.28	98.47	43.87	97.56	56.74	98.48
	Sg-CityU (ours)	Point Cloud + Scene Graph	**80.95**	**98.86**	**50.75**	**98.66**	**63.94**	**98.81**	**78.46**	**98.76**	**50.50**	**98.45**	**63.76**	**98.68**

6.2.2 *Comparison with Indoor Models.*

We conduct the comparative experiments between Sg-CityU and models in indoor settings shown in Table 3. For SOTA model 3D-VisTA [4] in the indoor setting, Sg-CityU achieves 4.31% points improvement in sentence-wise (59.63% → 63.94%) and 7.02% points improvement city-wise (56.74% → 63.76%) in acc@1 and 0.44% points improvements in sentence-wise (98.37% → 98.81%) and 0.20% points improvements city-wise (98.48% → 98.68%) in acc@10. Compared to indoor MQA models, the efficiency of Sg-CityU is attributed to the scene graph, which offers a semantic and spatial representation of city-level outdoor scenes. This representation features sparse instances that encompass a wide range of city-level scenes.

To evaluate the generalization and robustness of indoor models and Sg-CityU in diverse city scenes, our research includes a comparative analysis of their performance across different cities. In this study, we assess the performance of the models used in indoor settings and Sg-CityU models under two different settings: city-wise and sentence-wise. In the city-wise evaluation, ScanQA achieves an accuracy of 47.33% for acc@1 and 86.45% for acc@10. These figures represent a decline in performance compared to the sentence-wise setting, where acc@1 decreases by 1.95% (49.28% → 47.33%) and acc@10 decreases by 1.89% (88.34% → 86.45%). Similar trends are observed in other indoor MQA models, with CLIP-Guided experiencing a decrease of 4.61% (51.55% → 46.94%), 3D-VLP a decrease of 2.98% (51.72% → 48.74%), and 3D-VisTA a decrease of 2.89% (59.63% → 56.74%). In contrast, Sg-CityU shows a decline of 0.18% in acc@1 (63.94% → 63.76%) and 0.13% in acc@10 (98.81% → 98.68%) when comparing the city-wise to the sentence-wise setting. These results show that our model exhibits generalization and robustness capabilities across diverse city-level scenes compared to the indoor models.

6.2.3 *Comparison in Multi-hop Questions.*

We conduct experiments on both multi-hop and single-hop questions, comparing the performance of baseline models and the proposed Sg-CityU model, as presented in Table 3. Our findings show that the multimodal LLMs with image input exhibit suboptimal performance in multi-hop questions, with an acc@1 of 10.33% and 9.84% in sentence-wise and city-wise evaluations, respectively, for LLaVA, and 9.76% and 9.78% for Qwen-VL. LLMs utilizing scene graphs demonstrate superior performance, with Qwen achieving 11.21% and 12.59% in sentence-wise and city-wise evaluations, respectively, and Llama-2 achieving 20.00% and 18.82%. However, supervised models achieve better performances. In multi-hop questions, ScanQA achieves 8.31% (20.00% → 28.31%) improvements in sentence-wise and 8.21% (18.82% → 27.03%) improvements in city-wise compared to the best performance of general LLM. CLIP-Guided shows a 13.73% (20.00% → 33.73%) improvement in sentence-wise accuracy and a 13.59% (18.82% → 32.41%) improvement in city-wise accuracy. 3D-VLP achieves a 15.54% (20.00% → 35.54%) improvement in sentence-wise accuracy and a 16.13% (18.82% → 34.95%) improvement in city-wise accuracy. 3D-VisTA exhibits a 24.67% (20.00% → 44.67%) improvement in sentence-wise accuracy and a 25.05% (18.82% → 43.87%) improvement in city-wise accuracy. Similarly, our model Sg-CityU achieves an improvement of 30.75% (20.00% → 50.75%) in sentence-wise accuracy and 31.68% (18.82% → 50.50%) in city-wise accuracy compared to the best performance of general LLMs. We attribute this limitation to the domain gap between the training datasets of LLMs and the requirements for understanding city scenes. Therefore, LLMs cannot comprehend visual features in point clouds and the scene graph at the city level.

6.2.4 *Ablation Study in Sg-CityU.*

We conduct an ablation study to evaluate the effect of the scene graph on the performance of our proposed method Sg-CityU, as detailed in Table 4. When employing the scene graph as the input alone, Sg-CityU achieves 31.48% and 29.00% of acc@1 in sentence-wise and city-wise, 96.45% and 95.77% of acc@10 in sentence-wise and city-wise. These results indicate that Sg-CityU relying on the scene graph alone as input can not yield optimal performance and we attribute the absence of visual features. When utilizing the point cloud as the input alone, Sg-CityU achieves 52.25% and 49.01% of acc@1 in sentence-wise and city-wise, 98.07% and 97.40% of acc@10 in sentence-wise and city-wise. When employing the scene graph as assistance, Sg-CityU achieves 11.69% points improvement in sentence-wise (52.25% → 63.94%) and 14.75% points improvement city-wise (49.01% → 63.76%) in acc@1 and 0.61% points improvements in sentence-wise (98.07% → 98.68%) and 1.41% points improvements city-wise (97.40% → 98.81%) in acc@10. Incorporating scene graphs into the framework can enhance the performance of our proposed method Sg-CityU in City-3DQA tasks. This improvement is achieved by providing a more structured representation of city-level scenes, which facilitates an understanding of the spatial and semantic relationships between various instances.

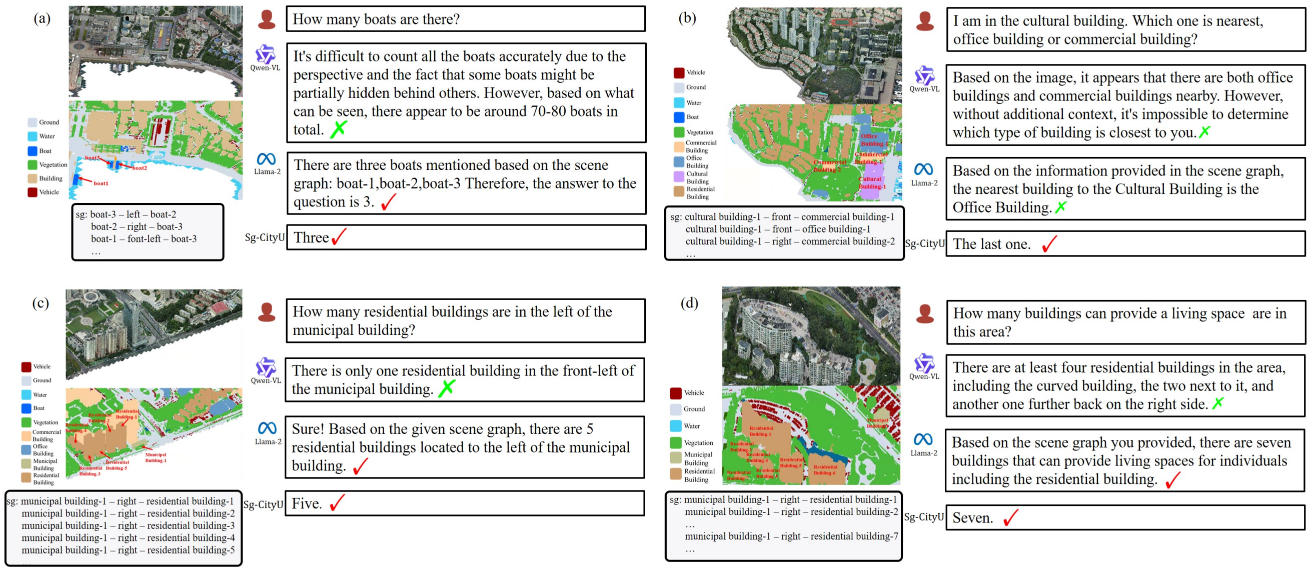

Figure 5: Visualization of examples. We compare and visualize the answer generated by Qwen-VL, Llama-2 and Sg-CityU. We visualize the city scene with the instance label and scene graph (sg). ✓ and ✗ mean the correct answer and wrong answer respectively.

Table 4: Ablation study on the input modal of Sg-CityU. This study specifically examines the effects of removing the point cloud and scene graph inputs while retaining the question input.

Input			Sentence-wise		City-wise	
Question	Scene Graph	Point Cloud	acc@1	acc@10	acc@1	acc@10
✓	✗	✓	52.25	98.07	49.01	97.40
✓	✓	✗	31.48	96.45	29.00	95.77
✓	✓	✓	**63.94**	**98.68**	**63.76**	**98.81**

6.3 Visualization and Case Study

We randomly select the cases and visualize them in Figure 5. In each case, we present the following components: the posed question, the scene with instance labels, and the corresponding scene graph. We compare the answers generated by three different models: the language-only LLM (Llama-2), the multimodal LLM (Qwen-VL), and the Sg-CityU model trained sentence-wise.

In **Case (a)**, we present the question, "*How many boats are there?*" Qwen-VL produces inaccurate answers due to a domain gap between its training datasets, which consist of 2D images sourced from the Internet, and the 3D point cloud images it encounters in the application. This gap leads to hallucinated answers. In contrast, Llama-2 based on the scene graph and Sg-CityU comprehends this city scene. In **Case (b)**, we pose the question, "*I am in the cultural building. Which one is nearest, the office building or commercial building?*" Both Qwen-VL and Llama-2 generate incorrect answers. We attribute this to the deficiency in the LLM's understanding of geographic scale information within the visual features. Scene graphs used in LLMs lack information regarding the distances between instances, leading to hallucinated answers. In **Case (c)**, we investigate the query, *"How many residential buildings are located to the left of the municipal building?"*. Llama-2 generates accurate responses, whereas Qwen-VL generates incorrect ones. We attribute it to the fact that LLMs based on scene graphs can leverage the relative spatial position within a scene graph for specific instances. In contrast, multimodal LLMs cannot comprehend the concept of *"left"* within the city scene using projection 2D images. In **Case (d)**, we pose the question, "*How many buildings can provide a living space in this area?* " Qwen-VL can detect the curved building as a residential building however, it can not detect the other dense and small residential buildings, leading to incorrect answers.

7 CONCLUSION

In this work, we investigate the 3D multimodal question answering (MQA) task for city scene understanding from both dataset and method perspectives. Firstly, we introduce a large-scale dataset, **City-3DQA**, designed to encompass a wide range of urban activities, facilitating enhanced comprehension at the city level. Secondly, a scene graph enhanced city scene understanding method **Sg-CityU** is proposed to deal with the long-range connections and spatial inference challenges in city-level scene understanding. Experiments show that our proposed method outperforms the indoor MQA models and the large language models, showing robustness and generalization across different cities. To our knowledge, we are the first to explore the 3D MQA task for the city scene understanding in both the dataset and method aspects, which can promote the development of human-environment interaction within cities.

REFERENCES

[1] [n. d.]. Apple Vision Pro - Apple. https://www.apple.com/apple-vision-pro/.

[2] [n. d.]. Microsoft HoloLens | Mixed Reality Technology for Business. https://www.microsoft.com/en-us/hololens.

[3] Stanislaw Antol, Aishwarya Agrawal, Jiasen Lu, Margaret Mitchell, Dhruv Batra, C Lawrence Zitnick, and Devi Parikh. 2015. Vqa: Visual question answering. In *Proceedings of the IEEE international conference on computer vision*. 2425–2433.

[4] Daichi Azuma, Taiki Miyanishi, Shuhei Kurita, and Motoaki Kawanabe. 2022. ScanQA: 3D question answering for spatial scene understanding. In *proceedings of the IEEE/CVF conference on computer vision and pattern recognition*. 19129–19139.

[5] Jinze Bai, Shuai Bai, Yunfei Chu, Zeyu Cui, Kai Dang, Xiaodong Deng, Yang Fan, Wenbin Ge, Yu Han, Fei Huang, Binyuan Hui, Luo Ji, Mei Li, Junyang Lin, Runji Lin, Dayiheng Liu, Gao Liu, Chengqiang Lu, Keming Lu, Jianxin Ma, Rui Men, Xingzhang Ren, Xuancheng Ren, Chuanqi Tan, Sinan Tan, Jianhong Tu, Peng Wang, Shijie Wang, Wei Wang, Shengguang Wu, Benfeng Xu, Jin Xu, An Yang, Hao Yang, Jian Yang, Shusheng Yang, Yang Yao, Bowen Yu, Hongyi Yuan, Zheng Yuan, Jianwei Zhang, Xingxuan Zhang, Yichang Zhang, Zhenru Zhang, Chang Zhou, Jingren Zhou, Xiaohuan Zhou, and Tianhang Zhu. 2023. Qwen Technical Report. *arXiv preprint arXiv:2309.16609* (2023).

[6] Jinze Bai, Shuai Bai, Shusheng Yang, Shijie Wang, Sinan Tan, Peng Wang, Junyang Lin, Chang Zhou, and Jingren Zhou. 2023. Qwen-VL: A Versatile Vision-Language Model for Understanding, Localization, Text Reading, and Beyond. *arXiv preprint arXiv:2308.12966* (2023).

[7] Andrew Ka-Ching Chan. 2016. Tackling global grand challenges in our cities. *Engineering* 2, 1 (2016), 10–15.

[8] Zhenyu Chen, Ali Gholami, Matthias Nießner, and Angel X Chang. 2021. Scan2cap: Context-aware dense captioning in rgb-d scans. In *Proceedings of the IEEE/CVF conference on computer vision and pattern recognition*. 3193–3203.

[9] Angela Dai, Angel X Chang, Manolis Savva, Maciej Halber, Thomas Funkhouser, and Matthias Nießner. 2017. Scannet: Richly-annotated 3d reconstructions of indoor scenes. In *Proceedings of the IEEE conference on computer vision and pattern recognition*. 5828–5839.

[10] Abhishek Das, Samyak Datta, Georgia Gkioxari, Stefan Lee, Devi Parikh, and Dhruv Batra. 2018. Embodied question answering. In *Proceedings of the IEEE conference on computer vision and pattern recognition*. 1–10.

[11] Samyak Datta, Sameer Dharur, Vincent Cartillier, Ruta Desai, Mukul Khanna, Dhruv Batra, and Devi Parikh. 2022. Episodic memory question answering. In *Proceedings of the IEEE/CVF Conference on Computer Vision and Pattern Recognition*. 19119–19128.

[12] Yasaman Etesam, Leon Kochiev, and Angel X Chang. 2022. 3dvqa: Visual question answering for 3d environments. In *2022 19th Conference on Robots and Vision (CRV)*. IEEE, 233–240.

[13] Difei Gao, Ruiping Wang, Shiguang Shan, and Xilin Chen. 2022. Cric: A vqa dataset for compositional reasoning on vision and commonsense. *IEEE Transactions on Pattern Analysis and Machine Intelligence* 45, 5 (2022), 5561–5578.

[14] Yixuan Geng, Zhipeng Wang, Limin Jia, Yong Qin, Yuanyuan Chai, Keyan Liu, and Lei Tong. 2023. 3DGraphSeg: A unified graph representation-based point cloud segmentation framework for full-range highspeed railway environments. *IEEE Transactions on Industrial Informatics* (2023).

[15] Mark A. Goddard, Zoe G. Davies, Solène Guenat, Mark J. Ferguson, Jessica C. Fisher, Adeniran Akanni, Teija Ahjokoski, Pippin M. L. Anderson, Fabio Angeoletto, Constantinos Antoniou, Adam J. Bates, Andrew Barkwith, Adam Berland, Christopher J. Bouch, Christine C. Rega-Brodsky, Loren B. Byrne, David Cameron, Rory Canavan, Tim Chapman, Stuart Connop, Steve Crossland, Marie C. Dade, David A. Dawson, Cynnamon Dobbs, Colleen T. Downs, Erle C. Ellis, Francisco J. Escobedo, Paul Gobster, Natalie Marie Gulsrud, Burak Guneralp, Amy K. Hahs, James D. Hale, Christopher Hassall, Marcus Hedblom, Dieter F. Hochuli, Tommi Inkinen, Ioan-Cristian Ioja, Dave Kendal, Tom Knowland, Ingo Kowarik, Simon J. Langdale, Susannah B. Lerman, Ian MacGregor-Fors, Peter Manning, Peter Massini, Stacey McLean, David D. Mkwambisi, Alessandro Ossola, Gabriel Pérez Luque, Luis Pérez-Urrestarazu, Katia Perini, Gad Perry, Tristan J. Pett, Kate E. Plummer, Raoufou A. Radji, Uri Roll, Simon G. Potts, Heather Rumble, Jon P. Sadler, Stevienna de Saille, Sebastian Sautter, Catherine E. Scott, Assaf Shwartz, Tracy Smith, Robbert P. H. Snep, Carl D. Soulsbury, Margaret C. Stanley, Tim Van de Voorde, Stephen J. Venn, Philip H. Warren, Carla-Leanne Washbourne, Mark Whitling, Nicholas S. G. Williams, Jun Yang, Kumelachew Yeshitela, Ken P. Yocom, and Martin Dallimer. 2021. A global horizon scan of the future impacts of robotics and autonomous systems on urban ecosystems. *Nature Ecology & Evolution* 5, 2 (01 Feb 2021), 219–230. https://doi.org/10.1038/s41559-020-01358-z

[16] J Vernon Henderson, Anthony J Venables, Tanner Regan, and Ilia Samsonov. 2016. Building functional cities. *Science* 352, 6288 (2016), 946–947.

[17] Qingyong Hu, Bo Yang, Sheikh Khalid, Wen Xiao, Niki Trigoni, and Andrew Markham. 2022. Sensaturban: Learning semantics from urban-scale photogrammetric point clouds. *International Journal of Computer Vision* 130, 2 (2022), 316–343.

[18] Zhao Jin, Munawar Hayat, Yuwei Yang, Yulan Guo, and Yinjie Lei. 2023. Context-aware alignment and mutual masking for 3d-language pre-training. In *Proceedings of the IEEE/CVF Conference on Computer Vision and Pattern Recognition*. 10984–10994.

[19] Jacob Devlin Ming-Wei Chang Kenton and Lee Kristina Toutanova. 2019. BERT: Pre-training of Deep Bidirectional Transformers for Language Understanding. In *Proceedings of NAACL-HLT*. 4171–4186.

[20] Ue-Hwan Kim, Jin-Man Park, Taek-Jin Song, and Jong-Hwan Kim. 2019. 3-D scene graph: A sparse and semantic representation of physical environments for intelligent agents. *IEEE transactions on cybernetics* 50, 12 (2019), 4921–4933.

[21] Thomas N Kipf and Max Welling. 2016. Semi-Supervised Classification with Graph Convolutional Networks. In *International Conference on Learning Representations*.

[22] Qi Kuang, Jinbo Wu, Jia Pan, and Bin Zhou. 2020. Real-time UAV path planning for autonomous urban scene reconstruction. In *2020 IEEE International Conference on Robotics and Automation (ICRA)*. IEEE, 1156–1162.

[23] Lik-Hang Lee, Tristan Braud, Simo Hosio, and Pan Hui. 2021. Towards augmented reality driven human-city interaction: Current research on mobile headsets and future challenges. *ACM Computing Surveys (CSUR)* 54, 8 (2021), 1–38.

[24] Weixin Liang, Youzhi Tian, Chengcai Chen, and Zhou Yu. 2020. Moss: End-to-end dialog system framework with modular supervision. In *Proceedings of the AAAI Conference on Artificial Intelligence*, Vol. 34. 8327–8335.

[25] Yiyi Liao, Jun Xie, and Andreas Geiger. 2022. Kitti-360: A novel dataset and benchmarks for urban scene understanding in 2d and 3d. *IEEE Transactions on Pattern Analysis and Machine Intelligence* 45, 3 (2022), 3292–3310.

[26] Liqiang Lin, Yilin Liu, Yue Hu, Xingguang Yan, Ke Xie, and Hui Huang. 2022. Capturing, reconstructing, and simulating: the urbanscene3d dataset. In *European Conference on Computer Vision*. Springer, 93–109.

[27] Haotian Liu, Chunyuan Li, Qingyang Wu, and Yong Jae Lee. 2024. Visual instruction tuning. *Advances in neural information processing systems* 36 (2024).

[28] Xiaojian Ma, Silong Yong, Zilong Zheng, Qing Li, Yitao Liang, Song-Chun Zhu, and Siyuan Huang. 2022. SQA3D: Situated Question Answering in 3D Scenes. In *The Eleventh International Conference on Learning Representations*.

[29] Taiki Miyanishi, Fumiya Kitamori, Shuhei Kurita, Jungdae Lee, Motoaki Kawanabe, and Nakamasa Inoue. 2023. CityRefer: Geography-aware 3D Visual Grounding Dataset on City-scale Point Cloud Data. In *Thirty-seventh Conference on Neural Information Processing Systems Datasets and Benchmarks Track*.

[30] Maria Parelli, Alexandros Delitzas, Nikolas Hars, Georgios Vlassis, Sotirios Anagnostidis, Gregor Bachmann, and Thomas Hofmann. 2023. Clip-guided vision-language pre-training for question answering in 3d scenes. In *Proceedings of the IEEE/CVF Conference on Computer Vision and Pattern Recognition*. 5606–5611.

[31] Charles R Qi, Or Litany, Kaiming He, and Leonidas J Guibas. 2019. Deep hough voting for 3d object detection in point clouds. In *proceedings of the IEEE/CVF International Conference on Computer Vision*. 9277–9286.

[32] Charles Ruizhongtai Qi, Li Yi, Hao Su, and Leonidas J Guibas. 2017. Pointnet++: Deep hierarchical feature learning on point sets in a metric space. *Advances in neural information processing systems* 30 (2017).

[33] Tianwen Qian, Jingjing Chen, Linhai Zhuo, Yang Jiao, and Yu-Gang Jiang. 2024. Nuscenes-qa: A multi-modal visual question answering benchmark for autonomous driving scenario. In *Proceedings of the AAAI Conference on Artificial Intelligence*, Vol. 38. 4542–4550.

[34] Nils Reimers and Iryna Gurevych. 2019. Sentence-BERT: Sentence Embeddings using Siamese BERT-Networks. In *Proceedings of the 2019 Conference on Empirical Methods in Natural Language Processing and the 9th International Joint Conference on Natural Language Processing (EMNLP-IJCNLP)*. 3982–3992.

[35] Elizabeth R Schotter. 2013. Synonyms provide semantic preview benefit in English. *Journal of Memory and Language* 69, 4 (2013), 619–633.

[36] Robyn Speer, Joshua Chin, and Catherine Havasi. 2017. Conceptnet 5.5: An open multilingual graph of general knowledge. In *Proceedings of the AAAI conference on artificial intelligence*, Vol. 31.

[37] Jiaxiang Tang, Xiaokang Chen, Jingbo Wang, and Gang Zeng. 2022. Point scene understanding via disentangled instance mesh reconstruction. In *European Conference on Computer Vision*. Springer, 684–701.

[38] Hugo Touvron, Louis Martin, Kevin Stone, Peter Albert, Amjad Almahairi, Yasmine Babaei, Nikolay Bashlykov, Soumya Batra, Prajjwal Bhargava, Shruti Bhosale, et al. 2023. Llama 2: Open foundation and fine-tuned chat models. *arXiv preprint arXiv:2307.09288* (2023).

[39] Denny Vrandečić and Markus Krötzsch. 2014. Wikidata: a free collaborative knowledgebase. *Commun. ACM* 57, 10 (2014), 78–85.

[40] Jan Oliver Wallgrün, Mahda M Bagher, Pejman Sajjadi, and Alexander Klippel. 2020. A comparison of visual attention guiding approaches for 360 image-based vr tours. In *2020 IEEE Conference on Virtual Reality and 3D User Interfaces (VR)*. IEEE, 83–91.

[41] Chenxi Whitehouse, Monojit Choudhury, and Alham Fikri Aji. 2023. LLM-powered Data Augmentation for Enhanced Cross-lingual Performance. In *The 2023 Conference on Empirical Methods in Natural Language Processing*.

[42] Erik Wijmans, Samyak Datta, Oleksandr Maksymets, Abhishek Das, Georgia Gkioxari, Stefan Lee, Irfan Essa, Devi Parikh, and Dhruv Batra. 2019. Embodied

question answering in photorealistic environments with point cloud perception. In *Proceedings of the IEEE/CVF Conference on Computer Vision and Pattern Recognition*. 6659–6668.

[43] Yi Wu, Yuxin Wu, Georgia Gkioxari, and Yuandong Tian. 2018. Building generalizable agents with a realistic and rich 3d environment. *arXiv preprint arXiv:1801.02209* (2018).

[44] Pengfei Xu, Xiaojun Chang, Ling Guo, Po-Yao Huang, Xiaojiang Chen, and Alexander G Hauptmann. 2020. A survey of scene graph: Generation and application. *IEEE Trans. Neural Netw. Learn. Syst* 1 (2020), 1.

[45] Xu Yan, Zhihao Yuan, Yuhao Du, Yinghong Liao, Yao Guo, Shuguang Cui, and Zhen Li. 2023. Comprehensive Visual Question Answering on Point Clouds through Compositional Scene Manipulation. *IEEE Transactions on Visualization & Computer Graphics* 01 (2023), 1–13.

[46] Guoqing Yang, Fuyou Xue, Qi Zhang, Ke Xie, Chi-Wing Fu, and Hui Huang. 2023. UrbanBIS: A Large-Scale Benchmark for Fine-Grained Urban Building Instance Segmentation. In *ACM SIGGRAPH 2023 Conference Proceedings*. 1–11.

[47] Shuquan Ye, Dongdong Chen, Songfang Han, and Jing Liao. 2022. 3D question answering. *IEEE Transactions on Visualization and Computer Graphics* (2022).

[48] Licheng Yu, Xinlei Chen, Georgia Gkioxari, Mohit Bansal, Tamara L Berg, and Dhruv Batra. 2019. Multi-target embodied question answering. In *Proceedings of the IEEE/CVF Conference on Computer Vision and Pattern Recognition*. 6309–6318.

[49] Han Zhang, Yucong Yao, Ke Xie, Chi-Wing Fu, Hao Zhang, and Hui Huang. 2021. Continuous aerial path planning for 3D urban scene reconstruction. *ACM Trans. Graph.* 40, 6 (2021), 225–1.

[50] Lichen Zhao, Daigang Cai, Jing Zhang, Lu Sheng, Dong Xu, Rui Zheng, Yinjie Zhao, Lipeng Wang, and Xibo Fan. 2022. Towards Explainable 3D Grounded Visual Question Answering: A New Benchmark and Strong Baseline. *IEEE Transactions on Circuits and Systems for Video Technology* (2022).

[51] Ziyu Zhu, Xiaojian Ma, Yixin Chen, Zhidong Deng, Siyuan Huang, and Qing Li. 2023. 3d-vista: Pre-trained transformer for 3d vision and text alignment. In *Proceedings of the IEEE/CVF International Conference on Computer Vision*. 2911–2921.